

# Harper-Hofstadter problem for 2D electron gas with k-linear Rashba spin-orbit coupling

V. YA. DEMIKHOVSKII<sup>1</sup> and A. A. PEROV<sup>1</sup>

<sup>1</sup> *Nizhny Novgorod State University - Gagarin ave., 23, Nizhny Novgorod 603950, Russian Federation*

PACS. 71.70.Di – Landau levels.

PACS. 71.70.Ej – Spin-orbit coupling, Zeeman and Stark splitting, Jahn-Teller effect.

**Abstract.** – The Harper-Hofstadter problem for two-dimensional electron gas with Rashba spin-orbit coupling subject to periodic potential and perpendicular magnetic field is studied analytically and numerically. The butterfly-like energy spectrum, spinor wave functions as well as the spin density and average spin polarization are calculated for actual parameters of semiconductor structure. Our calculations show that in two-dimensional electron gas subject to periodic potential and uniform magnetic field the effects of energy spectrum splitting caused by large spin-orbit Rashba coupling can be observed experimentally.

*Introduction.* – The problem of quantum states of an electron subject to both periodic potential and homogeneous magnetic field remains to be actual for several last decades. There are various approaches and models for periodic potential and different approximations which are used for investigations of these states (see, ref. [1]). However, the spin-orbit interaction is usually excluded from the models as well as the Zeeman term. Such approach can be justified as long as the amplitude of the periodic potential is big enough to make the Landau level splitting much greater than the typical spin-orbit coupling energy and the Zeeman term. At the same time, under the realistic experimental conditions with 2D electron gas subject to the potential of lateral superlattice the potential amplitude  $V_0$  can be of the same order as the spin-orbit (SO) Rashba coupling. For example, in recent papers [2,3] where a pioneering step into experimental observation of 2D magnetic Bloch states has been done, the magnitude of  $V_0$  was around 1-5 meV. In semiconductor structures with large SO coupling [4] the typical splitting energy can be of the same order as  $V_0$ .

In this paper we study magnetic Bloch states of 2D electrons subject to both periodic potential of a lateral superlattice and perpendicular magnetic field under the conditions when the SO coupling and Zeeman term should be taken into consideration. The energy band structure is calculated in the magnetic Brillouin zone (MBZ) and the magnetic Bloch states are constructed. Also, the spin density distribution in the elementary cell is obtained and the average spin polarization in a state with given quasimomentum are calculated. It is shown that the consideration of spin-orbit coupling is necessary for interpretation of realistic experiments.

*Hamiltonian matrix structure, energy band spectrum and wavefunctions.* – We consider 2D electron gas with spin-orbit Rashba coupling in a potential  $V(x, y)$  which is periodic in plane with the period  $a$ , and in a uniform magnetic field  $\mathbf{H}$  perpendicular to the plane of the electrons. The correspondent one-electron Hamiltonian has the following form:

$$\hat{H} = \hat{H}_0 + V(x, y), \quad (1)$$

where  $V(x, y) = V(x + na, y + ma)$  is a periodic potential,

$$\hat{H}_0 = (\hat{\mathbf{p}} - e\mathbf{A}/c)^2/2m^* + \frac{\alpha}{\hbar} \left( \hat{\sigma}_x(\hat{p}_y - eA_y/c) - \hat{\sigma}_y\hat{p}_x \right) - g\mu_B H \hat{\sigma}_z$$

is the Rashba Hamiltonian of an electron in uniform magnetic field [5, 6]. Here,  $\hat{p}_{x,y}$  are the momentum operator components,  $m^*$  is the electron effective mass,  $\hat{\sigma}$  are the Pauli matrices,  $\alpha$  is the parameter of the SO coupling,  $g$  is the Zeeman factor, and  $\mu_B$  is the Bohr magneton. We use the Landau gauge in which the vector potential has the form  $\mathbf{A} = (0, Hx, 0)$  and consider the potential  $V(x, y) = V_0(\cos(2\pi x/a) + \cos(2\pi y/a))$ . The quantum states structure of the system under consideration depends crucially on the parameter  $\Phi/\Phi_0 = p/q = |e|Ha^2/2\pi\hbar c$  ( $p$  and  $q$  are prime integers) which is the number of flux quanta per unit cell, and  $\Phi_0$  is the flux quanta.

One can express the eigenfunction of Hamiltonian (1) as a set of Landau wave functions in the presence of the SO coupling [7]. If we take  $p/q$  to be the rational number, the two-component magnetic Bloch function, analogous to the one-component magnetic Bloch function of the paper [1], can be written in the form

$$\begin{aligned} \Psi_{\mathbf{k}}(x, y) = & \begin{pmatrix} \Psi_{1\mathbf{k}}(x, y) \\ \Psi_{2\mathbf{k}}(x, y) \end{pmatrix} = \sum_{S=1}^{\infty} \sum_{n=1}^p \sum_{\ell=-\infty}^{+\infty} e^{ik_y y} e^{ik_x(\ell qa + nqa/p)} e^{2\pi i y(\ell p + n)/a} \times \\ & \times \left[ A_{0n}(\mathbf{k}) \psi_{0n\ell\mathbf{k}}^+(x, y) + A_{Sn}(\mathbf{k}) \psi_{Sn\ell\mathbf{k}}^+(x, y) + B_{S+1,n}(\mathbf{k}) \psi_{S+1,n\ell\mathbf{k}}^-(x, y) \right], \end{aligned} \quad (2)$$

where the spinors  $\psi_{0n\ell\mathbf{k}}^+ = \exp(ik_y y) \begin{pmatrix} 0 \\ \phi_0[\xi_{\ell n}] \end{pmatrix}$ ,  $\psi_{Sn\ell\mathbf{k}}^+ = \frac{\exp(ik_y y)}{\sqrt{1+D_S^2}} \begin{pmatrix} D_S \phi_{S-1}[\xi_{\ell n}] \\ \phi_S[\xi_{\ell n}] \end{pmatrix}$  and  $\psi_{Sn\ell\mathbf{k}}^- = \frac{\exp(ik_y y)}{\sqrt{1+D_S^2}} \begin{pmatrix} \phi_{S-1}[\xi_{\ell n}] \\ -D_S \phi_S[\xi_{\ell n}] \end{pmatrix}$  correspond to "+" and "-" branches of the spectrum of the Hamiltonian  $\hat{H}_0$  [7],  $D_S = (\sqrt{2S}\alpha/l_H)/(E_0^+ + \sqrt{(E_0^+)^2 + 2S\alpha^2/l_H^2})$ ,  $\phi_S[\xi]$  is the simple harmonic oscillator functions,  $l_H = c\hbar/|e|H$  is the magnetic length,  $E_0^+ = \hbar\omega_c/2 + g\mu_B H$  and  $\omega_c = |e|H/m^*c$  is the cyclotron frequency. Here quantum numbers  $S = 1, 2, 3, \dots$  characterize the pair of "+" and "-" states  $E_S^\pm = S\hbar\omega_c \pm \sqrt{(E_0^+)^2 + 2S\alpha^2/l_H^2}$  of the unperturbed Hamiltonian  $\hat{H}_0$ ,  $\xi_{\ell n} = (x - x_0 - \ell qa - nqa/p)/l_h$ ,  $x_0 = c\hbar k_y/|e|H$ .

Note that the spinor wave function (2) is the eigenfunction of both the Hamiltonian (1) and operator of magnetic translation and therefore it have to obey the following Bloch-Peierls conditions

$$\Psi_{\mathbf{k}}(x + qa, y + a) = \Psi_{\mathbf{k}}(x, y) \exp(ik_x qa) \exp(ik_y a) \exp(2\pi i y/a),$$

where  $\mathbf{k}$  is quasimomentum defined in the MBZ

$$-\pi/qa \leq k_x \leq \pi/qa, \quad -\pi/a \leq k_y \leq \pi/a.$$

So, the magnetic Brillouin zone is the same as for charged spinless particle. At the limit of high magnetic fields the functions  $\psi_{Snl\mathbf{k}}^+$  and  $\psi_{Snl\mathbf{k}}^-$  are proportional to eigenspinors of Pauli operator  $\hat{\sigma}_z$ :  $\begin{pmatrix} 1 \\ 0 \end{pmatrix}$  and  $\begin{pmatrix} 0 \\ 1 \end{pmatrix}$ .

Substituting eq.(2) in the Schrödinger equation  $\hat{H}\Psi = E\Psi$  we come to the infinite system of linear equations for coefficients  $A_{Sn}(\mathbf{k})$  and  $B_{Sn}(\mathbf{k})$ . In the case when periodic potential amplitude and spin-orbit coupling energy have the same order and the inequality  $\Delta E_{SO} \simeq V_0 \leq \hbar\omega_c$  takes place the system of linear equations can be reduced to the system of infinite number of uncoupled groups of  $2p$  equations. Each group describes the magnetic Bloch states formed from the states with energies  $E_S^+$  and  $E_{S+1}^-$  of the single Landau level split by SO interaction.

In this approximation the system of  $2p$  linear equations attached to the quantum number  $S$  is defined by the following Hamiltonian matrix

$$H_{nn'}^{SS'} = \begin{pmatrix} G_1 & M & 0 & \dots & 0 & M^* & F_1 & J & 0 & \dots & 0 & T^* \\ M^* & G_2 & M & 0 & \dots & 0 & T & F_2 & J & 0 & \dots & 0 \\ \dots & \dots & \dots & \dots & \dots & \dots & \dots & \dots & \dots & \dots & \dots & \dots \\ M^* & 0 & \dots & 0 & M^* & G_p & J^* & 0 & \dots & 0 & T & F_p \\ F_1^* & T^* & 0 & \dots & 0 & J & U_1 & N & 0 & \dots & 0 & N^* \\ J^* & F_2^* & T^* & 0 & \dots & 0 & N^* & U_2 & N & 0 & \dots & 0 \\ \dots & \dots & \dots & \dots & \dots & \dots & \dots & \dots & \dots & \dots & \dots & \dots \\ T & 0 & \dots & 0 & J & F_p^* & N^* & 0 & \dots & 0 & N^* & U_p \end{pmatrix} \quad (3)$$

which has the block structure. In eq.(3) the matrix elements are defined as follows

$$\begin{aligned} G_n &= E_S^+ + V_0 e^{-\pi q/2p} \cos(2\pi x_0/a + 2\pi nq/p) [D_S^2 L_{S-1}^0(\pi q/p) + L_S^0(\pi q/p)] \frac{1}{1 + D_S^2}, \\ M &= \frac{V_0}{2} \exp(ik_x qa/p) e^{-\pi q/2p} [D_S^2 L_{S-1}^0(\pi q/p) + L_S^0(\pi q/p)] \frac{1}{1 + D_S^2}, \\ U_n &= E_{S+1}^- + V_0 e^{-\pi q/2p} \cos(2\pi x_0/a + 2\pi nq/p) [D_{S+1}^2 L_{S+1}^0(\pi q/p) + L_S^0(\pi q/p)] \frac{1}{1 + D_{S+1}^2}, \\ N &= \frac{V_0}{2} e^{ik_x qa/p} e^{-\pi q/2p} [D_{S+1}^2 L_{S+1}^0(\pi q/p) + L_S^0(\pi q/p)] \frac{1}{1 + D_{S+1}^2}, \\ F_n &= V_0 e^{-\pi \frac{q}{2p}} \sin(2\pi \frac{x_0}{a} + 2\pi \frac{nq}{p}) \left[ \frac{D_{S+1}}{\sqrt{S+1}} L_S^1(\pi q/p) - \frac{D_S}{\sqrt{S}} L_{S-1}^1(\pi q/p) \right] \frac{1}{(1 + D_S^2)(1 + D_{S+1}^2)}, \\ J &= \frac{V_0}{\sqrt{2}} e^{i \frac{k_x qa}{p}} e^{-\pi \frac{q}{2p}} \sqrt{\frac{\pi q}{2p}} \left[ \frac{D_{S+1}}{\sqrt{S+1}} L_S^1(\pi q/p) - \frac{D_S}{\sqrt{S}} L_{S-1}^1(\pi q/p) \right] \frac{1}{(1 + D_S^2)(1 + D_{S+1}^2)}, \\ T &= -\frac{V_0}{\sqrt{2}} e^{-i \frac{k_x qa}{p}} e^{-\pi \frac{q}{2p}} \sqrt{\frac{\pi q}{2p}} \left[ \frac{D_{S+1}}{\sqrt{S+1}} L_S^1(\pi q/p) - \frac{D_S}{\sqrt{S}} L_{S-1}^1(\pi q/p) \right] \frac{1}{(1 + D_S^2)(1 + D_{S+1}^2)}, \end{aligned} \quad (4)$$

Here  $L_S^K(z)$  is the Laguerre polynomial.

This system has a form of generalized Harper's equation. Matrix elements  $G_n$  and  $M$  in the left upper block of eq.(3) characterize the interaction between different states of the "+" branch and elements  $U_n$  and  $N$  in right low block are due to the interaction between states of the "-" branch. The right upper and left low blocks with elements  $F_n$ ,  $J$  and  $T$  describe the transition between states of the neighbor "+" and "-" branches with index  $S$ . Matrix elements in these four blocks are periodic in  $n$  with period  $p$ . So, each block has the size  $p \times p$ .

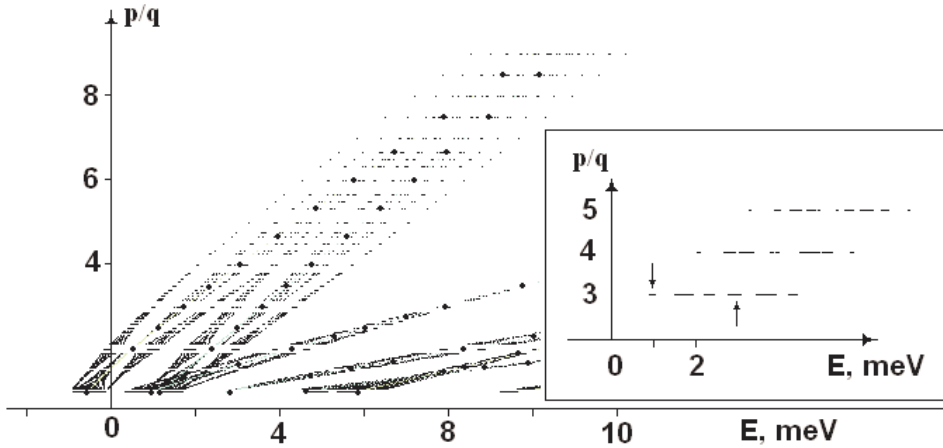


Fig. 1 – Position of energy subbands versus magnetic flux numbers at the parameters indicated in the text. The big dots show ”+” and ”-” Landau level positions in the absence of periodic potential. The insert shows  $2p$  energy subbands for  $p/q = 3/1, 4/1, 5/1$ .

Numerical calculations of energy spectrum and wave functions were carried out for the actual parameters which approximately correspond to the structure used in the experiment. In our calculations we used the following parameters of 2D electron gas:  $V_0 = 1 \text{ meV}$ , effective mass  $m^* = 0.05 m_0$ ,  $g = g_{\text{InAs}} = -2.0$ ,  $\alpha = 5 \cdot 10^{-11} \text{ eV} \cdot m$ . The lattice period was chosen as  $a = 60 \text{ nm}$  and  $V_0 = 1 \text{ meV}$ . Under these parameters the corresponding spectrum structure in magnetic field becomes well resolved and SO splitting is larger than Zeeman splitting at  $p/q \leq 5$ . The chosen parameters approximately correspond to the InAs quantum well where the Rashba SO constant can reach the maximal value  $5 \cdot 10^{-11} \text{ eV} \cdot m$  due to electron wave function penetration into barrier layer [4].

In fig.1 we show the electron energy levels for the state  $\mathbf{k} = 0$  versus the magnetic flux number. The big dots define the position of Landau levels  $E_S^\pm$  in the absence of periodic potential. The insert demonstrates the magnetic subbands at  $p/q$  equal to  $3/1, 4/1$  and  $5/1$  for  $\mathbf{k}$  located in the magnetic Brillouin zone. The upper arrow marks the lowest magnetic subband for which the dispersion law  $E_1(\mathbf{k})$  is plotted in fig.2. Note that the spectrum of magnetic subbands has the symmetry of the  $C_{4V}$  group, as it should be. As one can see from fig.1 the periodic potential forms the spectra which resemble the Hofstadter butterflies at the region  $1 \leq p/q \leq 2$ . For  $p/q \geq 3$  the magnetic subbands split by SO coupling and periodic potential are not overlapped. So, at magnetic fields corresponding to  $p/q \geq 3$  the unperturbed levels (fat dots in fig.1) are grouped into pairs and, therefore, our two-branch approximation is appropriate.

To compare the effects of level splitting due to the periodic potential as well as Zeeman effect and SO coupling we calculated the energy spectra formed from the lowest pair of Landau levels (see fig.3). In fig.3a we show the Hofstadter-like spectrum in the absence of Zeeman and SO interactions. Here, all levels are two-fold degenerate. At the presence of Zeeman interaction (fig.3b) the degeneracy is lifted and the correspondent spectrum is the superposition of two Hofstadter-like butterflies. Fig.3c demonstrates the splitting due to the SO Rashba coupling. So, under the parameters and magnetic fields indicated above the SO interaction is large enough to form two non-overlapped and non-degenerate groups of magnetic subbands.

We have calculated also the electron density  $|\Psi_{\mathbf{k}}(x, y)|^2 = |\Psi_{1\mathbf{k}}(x, y)|^2 + |\Psi_{2\mathbf{k}}(x, y)|^2$  at

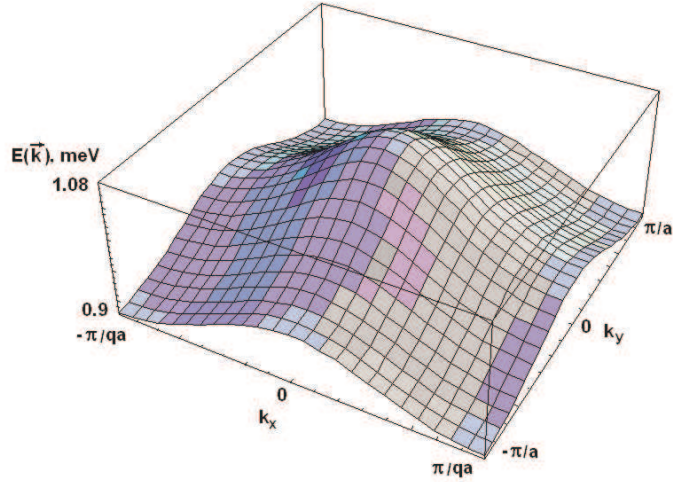


Fig. 2 – Electron energy versus quasimomentum in magnetic Brillouin zone.

$\mathbf{k} = 0$  for the fourth magnetic subband labelled by low arrow at the insert in fig.1. At the center of MBZ it has the symmetry of the  $C_{4V}$  group. Note, that for the state  $\mathbf{k} \neq 0$  the electron density does not possess the symmetry of the lattice.

*Spin density and average spin polarization.* – In the 2D electron gas with spin-orbit coupling at the presence of the periodic potential and perpendicular magnetic field the non-trivial spin structure appears in each of magnetic energy bands. Such a structure at a certain  $\mathbf{k}$  can be characterized by the vector field of the spin density in coordinate space

$$S_{i\mathbf{k}}(x, y) = \Psi_{\mathbf{k}}^{\dagger}(\mathbf{r})\hat{\sigma}_i\Psi_{\mathbf{k}}(\mathbf{r}), \quad (i = x, y).$$

In addition, spin states can be characterized by the average spin distribution in  $\mathbf{k}$  space

$$S_i(\mathbf{k}) = \langle S_{i\mathbf{k}}(x, y) \rangle = \langle \Psi_{\mathbf{k}}^{\dagger}(\mathbf{r})\hat{\sigma}_i\Psi_{\mathbf{k}}(\mathbf{r}) \rangle,$$

where the brackets mean the integration on  $x$  and  $y$  over the magnetic unit cell.

In fig.5 we show the spin density distribution calculated in the  $\mathbf{r}$ -space for the square superlattice with parameters indicated above. All results correspond to the fourth magnetic

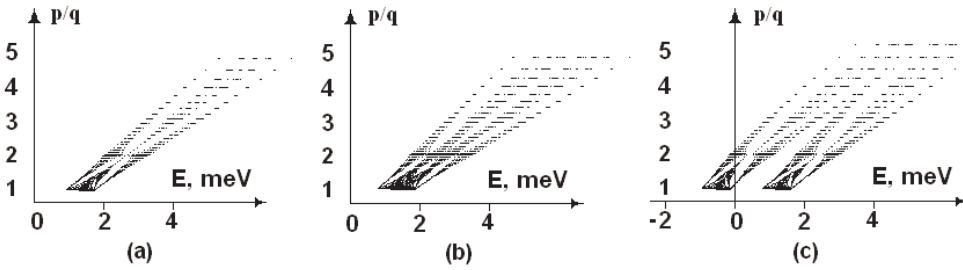


Fig. 3 – Energy spectra in the absence of SO Rashba coupling and Zeeman effect (a), in the presence of Zeeman splitting only (b), and when all of the contributions to level splitting are present (c). The parameters are the same as in fig.1.

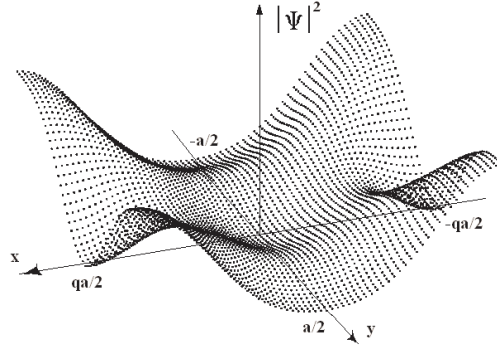


Fig. 4 – The electron density  $|\Psi_{\mathbf{k}}(x, y)|^2 = |\Psi_{1\mathbf{k}}(x, y)|^2 + |\Psi_{2\mathbf{k}}(x, y)|^2$  at  $\mathbf{k} = 0$  for the fourth magnetic subband.

energy band shown at the insert in fig.1 for the state  $\mathbf{k} = 0$ . The  $S_{x\mathbf{k}=0}(x, y)$  and  $S_{y\mathbf{k}=0}(x, y)$  densities have the  $C_s$  symmetry, but the  $S_{z\mathbf{k}=0}(x, y)$  component has the  $C_{4V}$  symmetry. The integration of the spin densities over the magnetic unit cell leads to the zero values of  $S_x(\mathbf{k})$  and  $S_y(\mathbf{k})$  at  $\mathbf{k} = 0$  (see fig.6a). The integration of  $S_{z\mathbf{k}=0}(x, y)$  over the magnetic unit cell results to the positive value of the average spin projection along magnetic field.

In fig.6 we show the average spin polarization in the MBZ for the fourth band at the magnetic flux  $p/q = 3/1$  (see fig.1). Fig.6a demonstrates the distribution of the components  $S_x(\mathbf{k})$  and  $S_y(\mathbf{k})$  and fig.6b shows the  $S_z(\mathbf{k})$  component. The distribution in fig.6a has the vortex structure with the  $C_2$  symmetry. The vortex centers are located at the center and at the corners of MBZ. These two vortices have opposite directions of rotation. In these points the average lateral spin components are smaller than perpendicular component  $S_z(\mathbf{k})$ . For the state  $\mathbf{k} = 0$  such a behavior is due to the small value of SO coupling in comparison

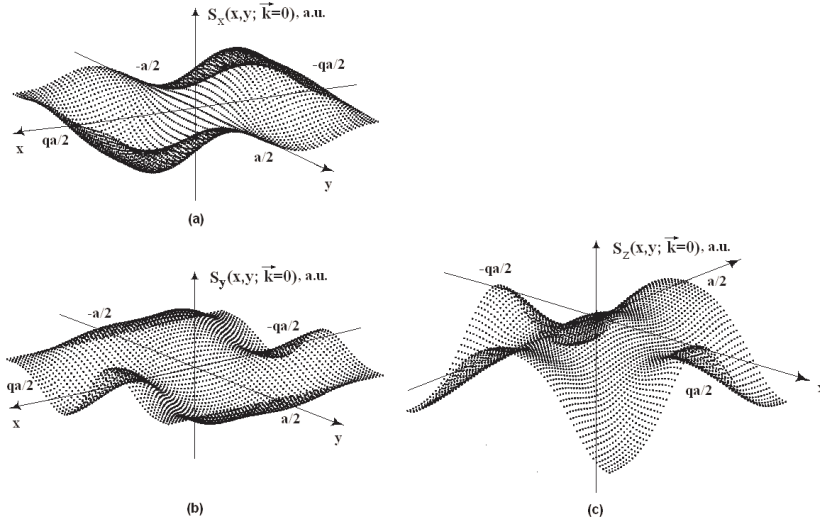


Fig. 5 – Electron spin densities in a unit cell of the lateral superlattice.

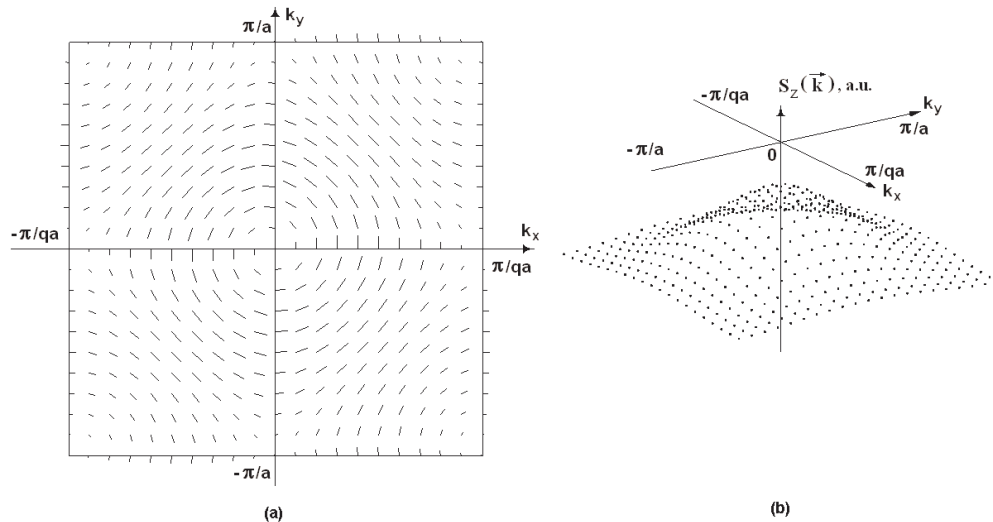


Fig. 6 – (a) Distribution of average spin polarization  $S_x(\mathbf{k})$  and  $S_y(\mathbf{k})$  in the fourth magnetic subband attached to the two lowest neighbor branches. (b)  $S_z(\mathbf{k})$  in the fourth magnetic energy subband.

with Zeeman effect. At the corners of MBZ the SO coupling is effectively smaller than the spin splitting in a magnetic field as a result of state mixing at the magnetic Brillouin zone edges. Here, in accordance with normalizing condition the  $|S_z(\mathbf{k})|$  component has the local maxima. We would like to note here that these spin vortices define the Berry phases and, respectively, the spin Hall conductance. Due to the same fact of state mixing by periodic potential the SO coupling effectively vanishes at the points where the edges of MBZ cross the  $k_x = 0$  and  $k_y = 0$  lines. Finally, note that the total magnetic moment of 2D electron gas which completely occupies this zone is positive.

*Conclusion.* – We have considered the effects of spin-orbit coupling on the quantum states of two-dimensional electron gas at the presence of periodic potential and uniform magnetic field. The Hofstadter butterfly-like energy band spectrum and electron density in the unit cell was analyzed. We demonstrate that the Zeeman interaction and the spin-orbit coupling form a complex and intricate spin periodic structure in the field of the lateral superlattice. The electron spin densities  $S_{x\mathbf{k}}(x, y)$ ,  $S_{y\mathbf{k}}(x, y)$  and  $S_{z\mathbf{k}}(x, y)$  as well as average spin polarizations  $S_x(\mathbf{k})$ ,  $S_y(\mathbf{k})$  and  $S_z(\mathbf{k})$  for the states with different quasimomentum  $\mathbf{k}$  defined in magnetic Brillouin zone were calculated and the role of three contribution to the spin orientation was investigated. We think that our results will be useful for analyzing the data of real experiments on the hunting of Hofstadter butterfly in two-dimensional electron gas.

\*\*\*

This work was supported by the program of Russian Ministry of Education and Science: Development of scientific potential of High School (project 2.1.1.2363), grant of Russian Foundation of Basic Research (no. 06-02-17189) and grant of the President of Russian Federation (MK-5165.2006.2).

## REFERENCES

- [1] THOULESS D.J., KOHMOTO M., NIGHTINGALE M.P. ET AL, *Phys. Rev. Lett.*, **49** (1982) 405.
- [2] ALBRECHT C., SMET J.H., K. VON KLITZING ET AL, *Phys. Rev. Lett.*, **86** (2001) 147.
- [3] GEISEL M.C., SMET J.H., UMANSKY V. ET AL, *Phys. Rev. Lett.*, **92** (2004) 256801.
- [4] GRUNDLER D., *Phys. Rev. Lett.*, **84** (2000) 6074.
- [5] BYCHKOV YU.A., RASHBA E.I., *JETP Lett.*, **39** (1984) 78.
- [6] BYCHKOV YU.A., MEL'NIKOV V.I. and RASHBA E.I., *ZhETF*, **98** (1990) 717.
- [7] WANG X.F., VASILOPOULOS P., *Phys. Rev. B*, **67** (2003) 085313.
- [8] CHANG M.-C., *Phys. Rev. B*, **71** (2005) 085315.
- [9] DEMIKHOVSKII V.YA., KHOMITSKY D.V., *Pis'ma v ZhETF*, **83** (2006) 399.
- [10] DEMIKHOVSKII V.YA., KHOMITSKY D.V., *cond-mat/0603364*, (2006) , unpublished.